JOURNAL OF MATERIALS SCIENCE **36** (2001) 3549–3555

Characterization of the protective effect of aluminium surface treatments by d.c. and a.c. measurements

J.-P. DASQUET
Laboratoire de Chimie des Matériaux Inorganiques et Energétiques, Université Paul Sabatier - UMR CNRS n°5070 118, route de Narbonne, 31062 Toulouse cedex, France
E-mail: jpdasquet@yahoo.fr

D. CAILLARD
Centre d'Elaboration des Matériaux et d'Etudes Strucrurales, UP 8011 29, rue Jeanne Marvig BP 4347 31055 Toulouse cedex, France

J.-P. BONINO, R. S. BES
Laboratoire de Chimie des Matériaux Inorganiques et Energétiques, Université Paul Sabatier - UMR CNRS n°5070 118, route de Narbonne, 31062 Toulouse cedex, France

Steady-state and electrochemical impedance spectroscopy measurements have been made on anodic layers on 1050 and 2024T3 aluminium alloys prepared from solutions of phosphoric acid, boric acid and sodium tetraborate, before and after impregnation treatment with zinc. Corrosion characteristics of the anodic layers were dependent on the aluminium substrate and the electrolyte. Aluminium alloy composition was found to be the most important factor for corrosion resistance; alloying elements of 2024T3 alloy (like copper) had a harmful influence on this layer property. Steady-state measurements allowed the oxide layer behaviour to be studied in the anodic range by the determination of an anodic passivity domain. This domain was characterized by a weak aluminium oxidation through the oxide layer. The zinc impregnation treatment had a marked protective effect on each studied anodic layer. This treatment can be used as an alternative to hot sealing in water or chromic acid solution.

1. Introduction

An important treatment used for the protective, decorative or adhesive surface treatment of aluminium is anodic oxidation. Anodizing consists of the controlled electrochemical growth of an aluminium oxide film by the anodic polarization of the aluminium substrate in a particular electrolyte solution. In neutral solutions such as boric acid, the native oxide film at the surface develops to a compact and uniform oxide layer, commonly called the barrier layer [1–3]. In aggressive solutions such as phosphoric and sulphuric acids, a thick and porous film is also formed [1–4]. The dimension and properties of both type layers depend on the formation conditions, i.e. substrate and electrolyte composition, formation current density and temperature [5]. In a previous paper [6], influence of the aluminium substrate and electrolyte composition on the layer morphology was studied using transmission electron microscopy and a.c. impedance measurements. Porous layer morphology was shown to be very dependent on the aluminium substrate; electrolyte composition had a strong influence on the barrier and porous layer thickness.

The corrosion properties of anodized aluminium alloys are frequently increased by hot sealing in water or chromic acid solution. Some authors [7, 8] have reported that the porous oxide layer can be modified by impregnation with metallic compounds under alternating voltage (50 Hz), but the effect of this impregnation treatment on the electrochemical properties have not been studied.

The aim of this paper is first, to study the influence of anodic layer formation conditions (substrate and electrolyte composition) on its protective effect, and second, to study the effect of impregnation treatment with zinc on the electrochemical properties of the modified oxide layer. Results were obtained by electrochemical d.c. and a.c. measurements performed in a corrosive medium.

2. Experimental method

Before treatment, the aluminium alloys, 1050 (99.35 wt% Al, 0.4% Fe, 0.25% Si) and 2024T3 (Al, 4.4% Cu, 1.5% Mg, 0.6% Mn) were etched in alkaline solution at 60°C followed by acid etching in a sulphuric acid/iron sulphate solution at 60°C. Anodization was carried out in three different solutions: PAO : H_3PO_4 solution (0.8 mol.L^{-1}) under d.c. 15 V for 15 min. at room temperature; BAAO : H_3BO_3

($10\ g \cdot L^{-1}$) and H_2SO_4 ($40\ g \cdot L^{-1}$) solution under d.c. 15 V for 20 min. at room temperature; BBAO: $Na_2B_4O_7$ solution ($30\ g \cdot L^{-1}$) under d.c. 20 V for 20 min. at 65°C. Each of these operations was followed by a washing in deionised water. Impregnation was carried out in a zinc sulphate based electrolyte ($ZnSO4 : 30\ g \cdot L^{-1}$, $H_3BO_3 : 20\ g \cdot L^{-1}$, $MgSO_4 : 20\ g \cdot L^{-1}$, $(NH_4)_2SO_4 : 20\ g \cdot L^{-1}$), at room temperature with an alternating voltage (50 Hz) of varying amplitude between the working electrode and an inert auxiliary Ni electrode. The microstructure of the layers was observed by transmission electron microscopy (TEM); cross sections were prepared by ion milling and observed in a JEOL 2010 HC operated at 200 kV. The polarization curves and electrochemical impedance spectroscopy study were carried out in a thermostated cell containing 0.2 M NaCl/0.2 M Na_2SO_4 solution, using the conventional three electrode configuration. The impedance spectra were recorded on a Solartron 1250 frequency response analyser.

3. Results and discussion

3.1. Microstructural study of the anodic oxide layers

Aluminium substrate has a strong influence on the porous layer morphology [6, 9]. As we can see for BAAO layer, the growth of the porous layer was anisotropically oriented for 1050 substrate layer (Fig. 1a); pores were perpendicular to the substrate. On the other hand, for 2024T3 substrate layer (Fig. 1b), pores were not unidirectional; the porous layer structure looked like a sponge. Similar results were found for the two other electrolytes [6]. In fact, alloying elements of 2024T3 alloy caused this morphological difference [10]. During anodization treatment, these alloying elements behaved according to their physico-chemical properties, playing thus a significant role in the anodic film growth. They did not allow a well defined structure to be obtained, like for 1050 substrate layers.

The thickness of the barrier (e_b) and porous (e_p) layers for each oxide film is reported in Table I. As we can see, aluminium substrate had a weak influence on porous and barrier layer thickness. These thicknesses are strongly influenced by the electrolyte.

3.2. Electrochemical study of the anodic oxide layers

3.2.1. Steady-state measurements

Fig. 2 shows the polarization curves obtained for the 2024T3 aluminium alloy before and after BAAO in the cathodic and anodic ranges. From the cathodic polarization curve (Fig. 2a), it was observed that anodic oxidation leaded to a decrease of the cathodic current density. By the Tafel method [11], a corrosion current density in the cathodic range J_{cc} could be determined with a satisfactory accuracy. The results for each oxide layer are presented in Table II. The best results (i.e. the lower J_{cc} value) were obtained for the BAAO layer.

TABLE II Corrosion current density in the cathodic range J_{cc} for 2024T3 substrate layers

	2024T3	BBAO	PAO	BAAO
j_{cc} ($\mu A.cm^{-2}$)	20 ± 1	16 ± 1	14 ± 1	12 ± 1

In the anodic range (Fig. 2b), the polarization curves showed a similar decrease of the anodic current density due to the anodic oxidation. However, the irregular shape of these curves did not allow the Tafel method to be used without an important incertitude on the determination of the corrosion current density in the anodic range. We then plotted J vs. E (and not $\log(J)$ vs. E). The curve obtained for BBAO layer is shown in Fig. 3. On this curve, a potential E_0 could be determined, which seemed to mark the transition between two oxidation kinetics. Up to E_0, anodic current density was low, whereas above this potential, it increased quickly.

The potential domain between the corrosion potential E_{corr} and E_0 was called passivity domain [12]:

$$\Delta E = E_0 - E_{corr}$$

This domain was characterized by weak anodic current densities. We compared the value of ΔE with that of J_{cc} for each anodic oxidation layer (Fig. 4). This figure showed good correlation between these two electrochemical data. It allowed a hierarchy to be established between the various anodic oxidation layers in term of corrosion resistance: best results were obtained for BAAO layer, then PAO and BBAO.

The results obtained for 1050 substrate layers are summarized in Fig. 5, which compares the evolution of J_{cc} vs. ΔE for both substrates. For 1050 substrate layers, J_{cc} was systematically lower and ΔE systematically higher than for 2024 substrate layers, implying a better corrosion resistance.

3.2.2. a.c measurements

The Nyquist diagram obtained for a PAO layer on 2024T3 aluminium alloy is shown in Fig. 6. It was characterized by a single capacitive loop representative of the electrochemical behaviour of the barrier layer [13]. Extrapolating this capacitive loop to the real axis, a polarization resistance R_p could be determined, which was

TABLE I Thickness of barrier layer (e_b) and porous layer (e_p) for each oxide film

	PAO 1050	BAAO 1050	BBAO 1050	PAO 2024T3	BAAO 2024T3	BBAO 2024T3
e_b (nm)	26 ± 3	20 ± 3	15 ± 3	24 ± 3	20 ± 4	14 ± 3
e_p (μm)	0.30 ± 0.05	1.00 ± 0.05	0.90 ± 0.05	0.25 ± 0.05	0.90 ± 0.05	0.70 ± 0.05

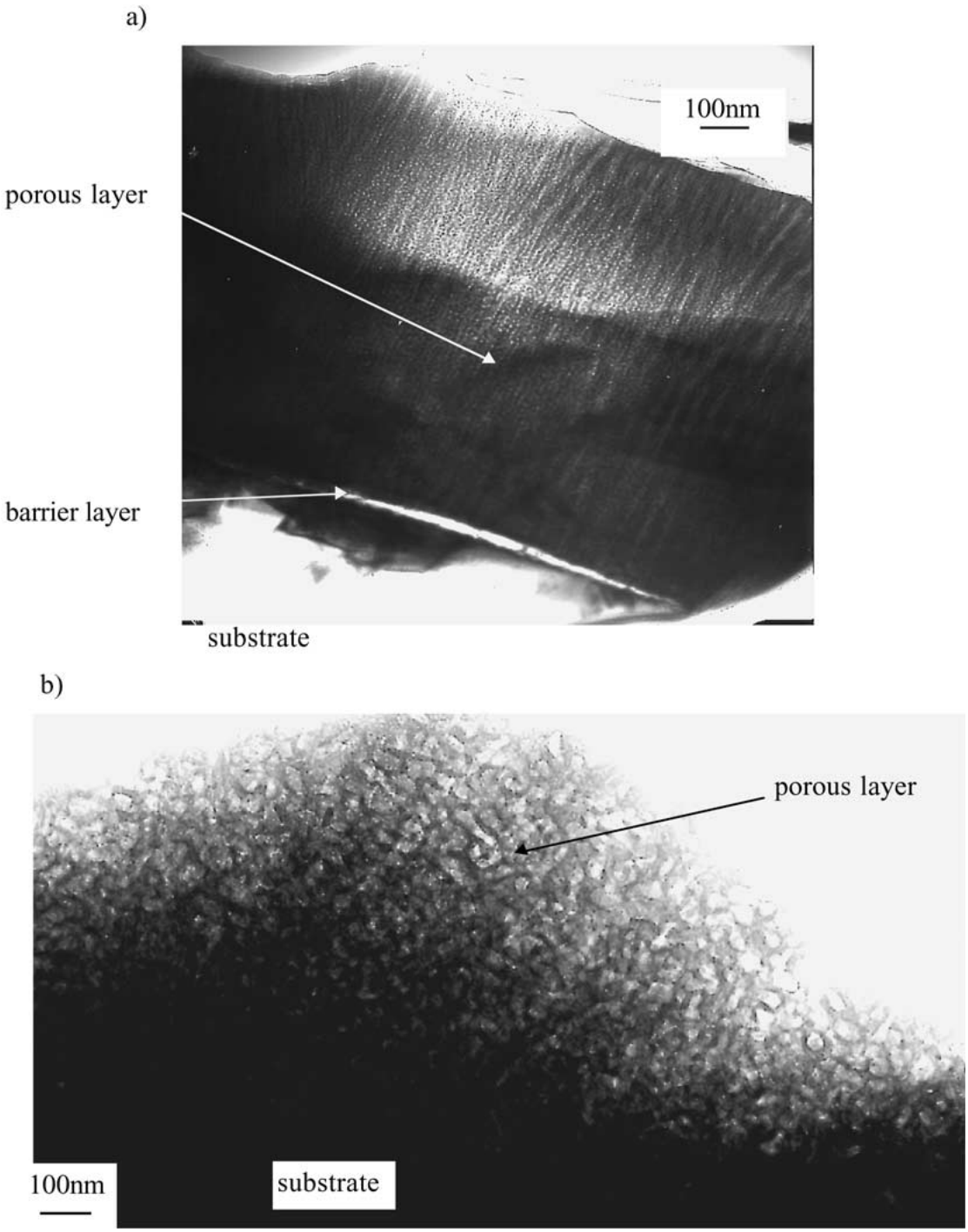

Figure 1 Cross section of a BAAO layer (TEM) on (a) 1050 and (b) 2024T3 substrates.

TABLE III Polarization resistance R_p determined by EIS for (a) 2024 and (b) 1050 substrate layers

	BBAO	PAO	BAAO
	a)		
$R_p(\Omega)$	8000	9730	17680
	b)		
$R_p(\Omega)$	24760	22140	52730

representative of a corrosion resistance [14]. The values obtained for both aluminium alloys are reported in Table III; they confirmed the hierarchy established with the steady-state measurements between the aluminium alloys and between the anodic oxidations studied.

The corrosion characteristics of 1050 substrate layers were better than that of 2024 substrate layers. In the case of 1050 substrate layers, the porous film presented a very well defined morphology, with unidirectional pores; on the contrary, the porous oxide structure obtained on 2024T3 substrate was disorganized. Nevertheless, it could not be concluded that the oxide layer morphology caused this electrochemical behaviour difference, because the 1050 alloy was known to have good corrosion properties, unlike the 2024T3. Indeed, alloying elements (like copper) of 2024T3 alloy were harmful for corrosion resistance.

The best results were obtained for the BAAO layers, which were the thickest anodic oxide layer. In the same way, it cannot be concluded that corrosion resistance

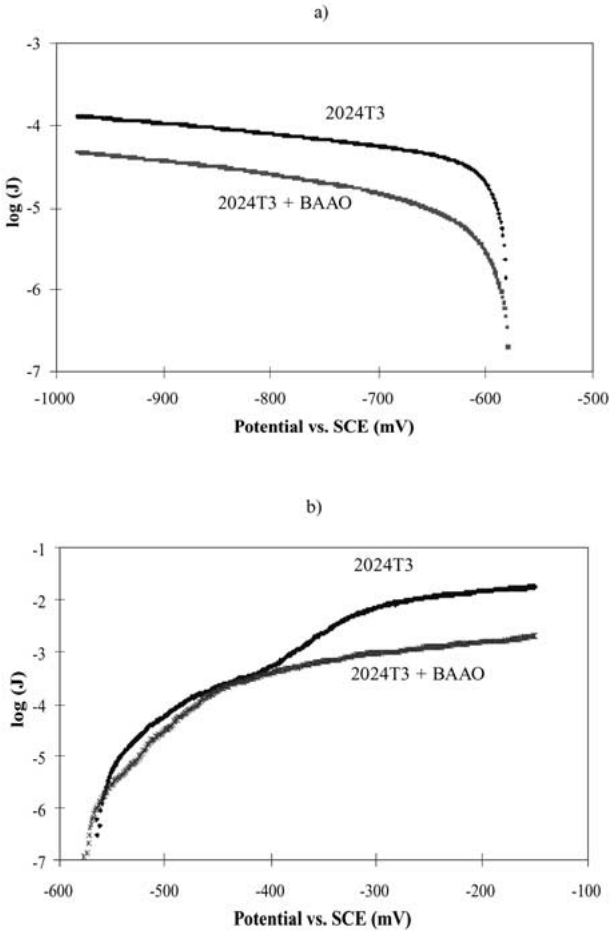

Figure 2 Polarization curve for the 2024T3 aluminium alloy before and after BAAO in the (a) cathodic and (b) anodic ranges.

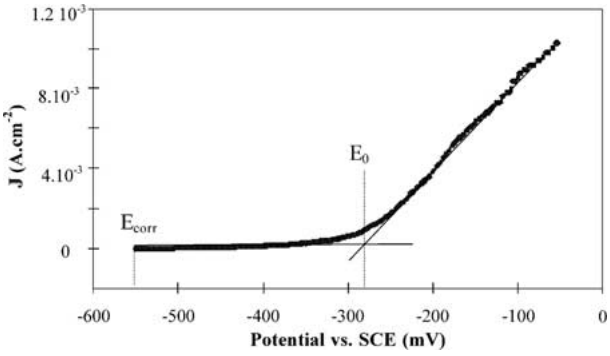

Figure 3 Polarization curve (J vs. E) for BBAO layer on 2024T3 alloy in the anodic range.

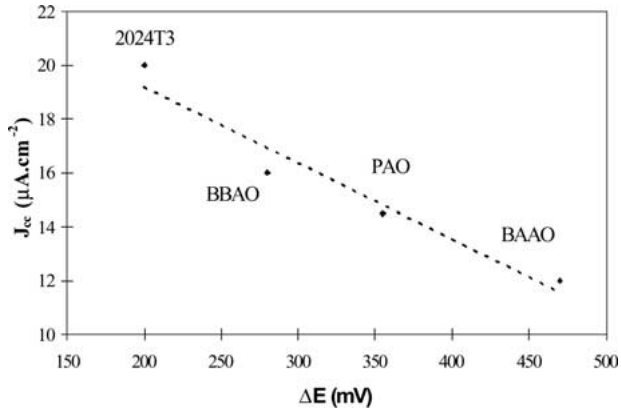

Figure 4 Corrosion current density in the cathodic range J_{cc} vs. passivity domain in the anodic range ΔE for 2024T3 substrate layers.

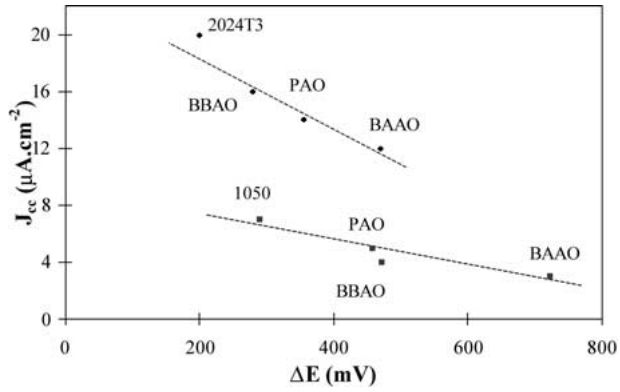

Figure 5 Corrosion current density in the cathodic range J_{cc} vs. passivity domain in the anodic range ΔE for 1050 and 2024T3 substrate layers.

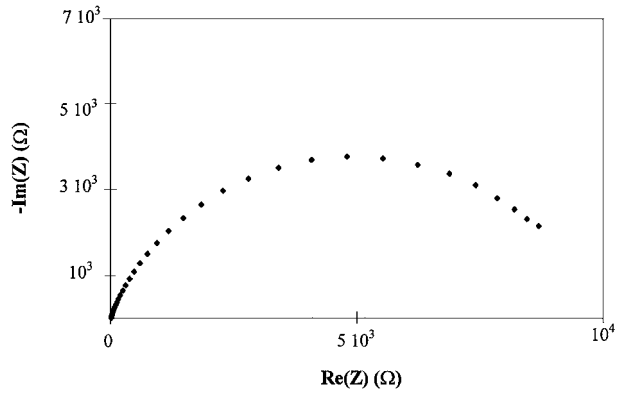

Figure 6 Nyquist diagram of a PAO layer on 2024T3 alloy.

increased with the oxide layer thickness, since the BBAO layers were relatively thick but had weak corrosion properties. Other factors have to be taken into account, like the layer porosity or the pore density.

We then studied the effect of the impregnation treatment on the oxide layer reactivity in corrosive medium.

3.3. Microstructural study of anodic layers impregnated with zinc

Impregnation treatment consists of the deposition of metal particles in the porous oxide layer under alternating voltage [9, 15, 12]. This treatment was generally used on 1050 alloy, after a phosphoric anodic oxidation PAO. We showed that it is also applicable on 2024T3 alloy, after BAAO and BBAO [12]. Usually, nickel was the impregnated element; in this case, only nickel metal was found in the oxide layer [15]. We studied zinc impregnation; we found that zinc was deposited under two states : zinc metal and zinc oxide [12]. As it can be supposed, the morphology of the layer obtained after anodic oxidation had a strong influence on the zinc deposit morphology. Fig. 7 shows PAO layers on 1050 and 2024T3 alloys impregnated with zinc. For both types of porous layer, the dark particles observed in a zone close to the substrate-oxide interface have been identified as microcristallized particles of zinc metal [9]. The growth of metal zinc in 1050 alloy layer (Fig. 7a) was oriented

by the anisotropy of the porosity and contributed to the formation of zinc needles, perpendicular to the substrate. In the 2024T3 alloy layer (Fig. 7b), metal grains do not have such a well defined morphology but were homogeneously distributed through the interfacial region of the oxide layer.

3.4. Electrochemical study of anodic oxide layers impregnated with zinc

3.4.1. Steady-state measurements

Fig. 8 shows the polarization curves of a BAAO layer on 2024T3 alloy before and after zinc impregnation. The protective effect of zinc impregnation was clearly shown by the decrease in anodic and cathodic currents. In particular, the decrease of anodic current resulted from the attenuation of aluminium oxidation through the oxide layer.

To quantify this protective effect, we defined an anodic inhibition rate η at corrosion potential plus 100 mV:

$$\eta = \frac{J_0 - J_i}{J_0}$$

where J_i was the anodic current density at corrosion potential +100 mV of the impregnated layer, J_0 was the

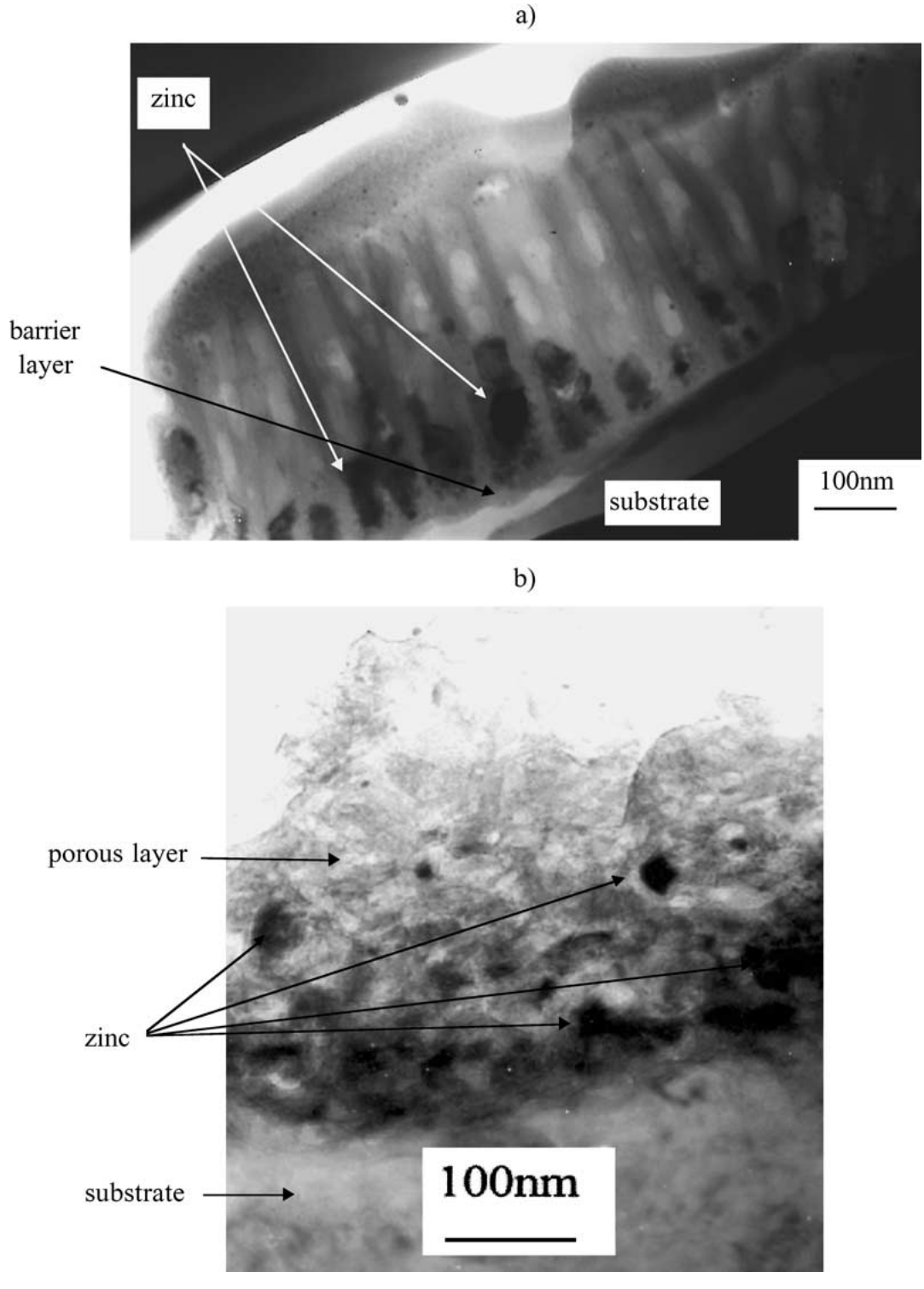

Figure 7 Cross section of PAO layers impregnated with zinc (TEM) on (a) 1050 alloy and (b) 2024T3 alloy.

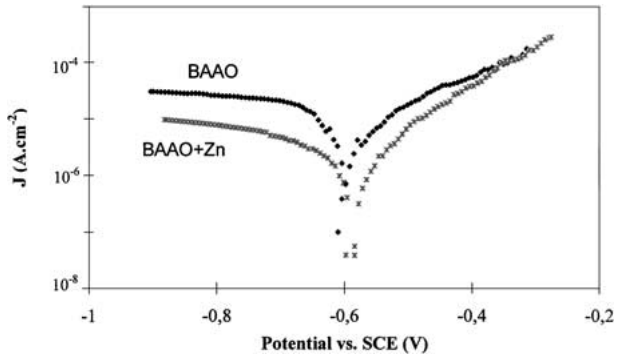

Figure 8 Polarization curves for a BAAO layer on 2024T3 alloy before and after zinc impregnation.

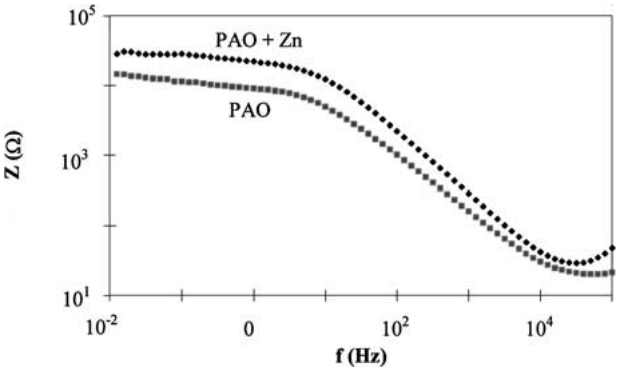

Figure 9 Bode diagram for a PAO layer on 2024T3 alloy before and after zinc impregnation.

anodic current density at corrosion potential +100 mV of the anodized layer.

Table IV presents results obtained for several impregnated layers. For each studied oxide layer, zinc impregnation treatment had a marked protective effect. However, results obtained for 1050 alloy layers were significatively better. So, deposit morphology seemed to influence layer reactivity; the more important protective effect was obtained for a well organized zinc deposit (1050 alloy).

To pursue this study, we followed the layer behaviour by electrochemical impedance spectroscopy.

3.4.2. a.c. measurements

From the Bode diagrams (Fig. 9 presents results obtained for a PAO layer on 2024T3 alloy), we determined the global resistance R_g of the impregnated layer [16] as the difference between the resistance values obtained at high and low frequencies (Table V). The increase in global resistance confirmed the protective effect of zinc impregnation, for the two aluminium alloys (1050 and 2024T3) and the three anodic oxidations (PAO, BAAO, BBAO).

TABLE IV Anodic inhibition rate η at corrosion potential +100 mV for various impregnated layers

	PAO 1050	PAO 2024T3	BBAO 2024T3	BAAO 2024T3
η(%)	85	76	65	70

TABLE V Global resistance before and after zinc impregnation for various oxide layers

	PAO 1050	PAO 2024T3	BAAO 2024T3	BBAO 2024T3
R_g(kΩ) before impregnation	38.8	14.5	28.3	8
R_g(kΩ) after impregnation	72.4	28.5	48	20.4

This impregnation treatment with zinc seemed to play a similar role to hot sealing. Zinc partially sealed the pores; moreover, its corrosion products, known to be voluminous, could also seal the pores.

4. Conclusion

Corrosion resistance of anodic oxidation layers on aluminium was found to be dependent on the aluminium substrate and on the electrolyte. For each type of studied anodic oxidation, corrosion characteristics determined by d.c. and a.c. measurements were better for 1050 substrate layers; alloying elements of 2024T3 alloy, like copper, were harmful for corrosion resistance. The electrochemical study allowed a hierarchy between the studied anodic oxidations to be established; best results in term of corrosion resistance were obtained for the BAAO layers. Although this layer was the thickest, this parameter was not sufficient to characterize corrosion resistance of the anodic layers. Other parameters had to be taken into account, like layer porosity and pore density.

The polarization curve study showed that Tafel method was not applicable in the anodic range; a passivity domain was then defined, which was in good agreement with the corrosion current density determined in the cathodic range by the Tafel method.

Zinc impregnation treatment had a strong effect on the anodic oxide layer reactivity in corrosive medium; it allowed corrosion resistance of the layers to be enhanced, for each aluminium substrate and each type of anodic oxidation. Zinc and its corrosion products seemed to partially seal the pores.

References

1. G. E. THOMPSON and G. C. WOOD, in "Treatise on Materials Science and Technology," Vol. 23 (Academic Press, London, 1983) ch. 5.
2. G. C. WOOD, J. P. O'SULLIVAN and B. VASZKO, *J. Electrochem. Soc.* **115** (1968) 618.
3. J. DE LAET, Thesis, Vrije Universiteit Brussel, Brussels, 1989.
4. R. M. A. AZZAM and N.M. BASHARA, "Ellipsometry and Polarized Light" (North Holland, Amsterdam, 1997).
5. J. P. O'SULLIVAN and G.C. WOOD, *Proc. R. Soc. London* **7317** (1970) 511.
6. J. P. DASQUET, D. CAILLARD, E. CONFORTO, J. P. BONINO and R. S. BES, *Thin Solid Films*, to be published.
7. C. R. MARTIN, *Science* **266** (1994) 1961.
8. T. SATO and S. SAKAI, *Trans. IMF* **57** (1979) 43.
9. J. P. DASQUET, J. P.BONINO, D. CAILLARD and R. S. BES, *J. Appl. Electrochem*, to be published.
10. H. HABAZAKI, K. SHIMIZU, P. SKELDON, G. E. THOMPSON, G. C. WOOD and X. ZHOU, *Trans. IMF* **75**(1) (1997) 18.

11. D. LANDOLT, "Corrosion et Chimie de Surface des Métaux" (Presses Polytechniques et Universités Romandes, Lausanne, 1993) p. 121.
12. J. P. DASQUET, Thesis, Toulouse III University, 1999.
13. J. VEREECKEN, Journées d'Electrochimie 99, Toulouse (1999) CT10-1.
14. J. J. BODU, M. BRUNIN, M. KEDDAM and H. TAKENOUTI, *Métaux Corrosion* (1997) 165.
15. J. SALMI, J. P. BONINO and R. S. BES, *this journal*, to be published.
16. J. HITZIG, K. JÜTTNER and W.J. LORENZ, *J. Elect. Soc.* **133**(5) (1986) 887.

Received 7 December 1999
and accepted 4 October 2000